

Towards the use of the most massive black hole candidates in AGN to test the Kerr paradigm

Cosimo Bambi*

*Arnold Sommerfeld Center for Theoretical Physics
Ludwig-Maximilians-Universität München, 80333 Munich, Germany*

(Dated: September 21, 2021)

The super-massive objects in galactic nuclei are thought to be the Kerr black holes predicted by General Relativity, although a definite proof of their actual nature is still lacking. The most massive objects in AGN ($M \sim 10^9 M_\odot$) seem to have a high radiative efficiency ($\eta \sim 0.4$) and a moderate mass accretion rate ($L_{\text{bol}}/L_{\text{Edd}} \sim 0.3$). The high radiative efficiency could suggest they are very rapidly-rotating black holes. The moderate luminosity could indicate that their accretion disk is geometrically thin. If so, these objects could be excellent candidates to test the Kerr black hole hypothesis. An accurate measurement of the radiative efficiency of an individual AGN may probe the geometry of the space-time around the black hole candidate with a precision comparable to the one achievable with future space-based gravitational-wave detectors like LISA. A robust evidence of the existence of a black hole candidate with $\eta > 0.32$ and accreting from a thin disk may be interpreted as an indication of new physics. For the time being, there are several issues to address before using AGN to test the Kerr paradigm, but the approach seems to be promising and capable of providing interesting results before the advent of gravitational wave astronomy.

PACS numbers: 98.54.Cm, 04.50.Kd, 98.62.Mw

I. INTRODUCTION

Gravity has been tested and verified for distances in the range ~ 1 mm to ~ 1 pc (mainly within its Newtonian limit) and for weak gravitational fields [1, 2]. The research is now moving to check the validity of the theory at cosmological scales, sub-millimeter distances, and for strong gravitational fields. One of the most intriguing predictions of General Relativity (GR) is that the collapsing matter produces singularities in the space-time. According to the weak cosmic censorship conjecture, singularities of gravitational collapse must be hidden within black holes (BHs) [3]. In 4-dimensional GR, uncharged BHs are described by the Kerr solution, which is completely specified by two parameters, the mass, M , and the spin angular momentum, J [4]. The condition for the existence of the event horizon is $a_* \leq 1$, where $a_* = |J/M^2|$ is the spin parameter¹. When $a_* > 1$, there is no horizon and the central singularity is naked, violating the weak cosmic censorship conjecture.

Astronomers have discovered at least two classes of BH candidates (for a review, see e.g. Ref. [5]): stellar-mass objects in X-ray binary systems ($M \sim 5 - 20 M_\odot$) and super-massive objects in galactic nuclei ($M \sim 10^5 - 10^9 M_\odot$). The estimates of the masses of these objects are robust, because determined via dynamical measurements and without any assumption about the geometry of the space-time. The key-point is that the stellar-mass objects in X-ray binary systems are too heavy to be neutron or quark stars for any reasonable matter equation of

state [6], while the super-massive objects at the centers of galaxies are too heavy, compact, and old to be clusters of non-luminous bodies, as the cluster lifetime would be shorter than the age of these systems [7]. All these objects are therefore thought to be the BHs predicted by GR, as they cannot be explained otherwise without introducing new physics. There are also some observations interpreted as an indirect evidence for the existence of the event horizon [8] (but see [9]). On the contrary, there is no indication that the geometry around these objects is described by the Kerr metric.

Testing the Kerr BH hypothesis is thus the next step to progress in this research field and several authors have indeed suggested possible ways to do it using present and future data (for a review, see e.g. Ref. [10]). A very promising approach is the detection of extreme mass ratio inspirals (EMRIs, i.e. systems consisting of a stellar-mass compact object orbiting a super-massive BH candidate) with future space-based gravitational-wave antennas. Missions like LISA will be able to follow the stellar-mass compact object for millions of orbits around the central super-massive BH candidate, and therefore deviations from the Kerr geometry will lead to a phase difference in the gravitational waveforms that grows with the number of observed cycles [11]. However, these data will not be available shortly, as the first mission will be at best in the early 2020s. The nature of BH candidates can also be tested by extending the methods currently used to estimate the spin of these objects, such as X-ray continuum [12] and $K\alpha$ -iron measurements [13], observations of quasi-periodic oscillations [14], and measurements of the cosmic X-ray background [15, 16]. These methods can in principle be applied even with present data, provided that the systematic errors are properly understood. Future observations of the shadow of nearby super-massive

* Cosimo.Bambi@physik.uni-muenchen.de

¹ Throughout the paper I use units in which $G_N = c = 1$, unless stated otherwise.

BH candidates are another exciting possibility to test the Kerr BH paradigm [17].

Previous studies have clearly pointed out that “rapidly-rotating” objects are the best candidates to test the Kerr BH hypothesis: if the object rotates fast, even a small deviation from the Kerr background can cause significant differences in the properties of the electromagnetic radiation emitted by the gas of the accretion disk and peculiar features, otherwise absent in the Kerr geometry, may show up [18, 19]. The aim of this paper is to investigate the potentialities of the most massive BH candidates in AGN, through the measurement of their radiative efficiency η , defined by $L_{\text{bol}} = \eta \dot{M}$, where L_{bol} is the bolometric luminosity of the source and \dot{M} is the mass accretion rate of the BH candidate. The estimate of the mean radiative efficiency of AGN through the Soltan’s argument [20] already suggests the presence of rapidly-rotating BHs [21, 22]. Recently, Davis and Laor have proposed a way to measure the radiative efficiency of individual AGN [23]. The authors found that the most massive BH candidates (with a mass $M \sim 10^9 M_{\odot}$) would have a high radiative efficiency, up to $\eta \sim 0.4$, and a moderate mass accretion rate, $L_{\text{bol}}/L_{\text{Edd}} \sim 0.3$, where L_{Edd} is the Eddington luminosity of the source. The standard accretion disk model in a Kerr background would predict a high value of the spin parameter a_* for these objects, extremely close to 1. At the same time, the moderate luminosity (in Eddington units) may indicate a thin accretion disk and the applicability of the standard accretion disk model. If these estimates and these considerations are correct, the most massive compact objects in AGN would be excellent candidates to test the Kerr paradigm. The sole measurement of η can potentially constrain either a_* and a deviation from the Kerr geometry.

The paper is organized as follows. In Section II, I review the standard accretion disk model, its assumptions and properties, its effects on the evolution of the spin parameter of the central object, and its applicability. In Section III, I consider an accretion disk in the Kerr background, summarizing well-known results that should be expected if the BH candidates are the BHs of GR. In Sections IV and V, I discuss accretion disks respectively in the Johannsen-Psaltis (JP) [24] and in the Manko-Novikov (MN) [25] space-times. These are two metrics that can be conveniently used to describe a background deviating from the Kerr geometry. The nature of the two metrics is definitively different: the JP metric describes non-Kerr BHs in a putative alternative theory of gravity, while the MN one is an exact solution of the Einstein’s vacuum equations and can describe the exterior gravitational field of generic compact objects. In both cases, the body is characterized by a mass, a spin angular momentum, and an infinite number of “deformation parameters”, even if here, for the sake of simplicity, I will consider only a single deformation parameter at a time. I will show that the two metrics present common features. In particular, a high radiative efficiency neces-

sarily requires a very rigid compact object, much stiffer than a self-gravitating fluid with “normal” equations of state. The confirmation of the existence of individual AGN with high radiative efficiency ($\eta > 0.3$) can potentially either be used to put strong constraints on the Kerr nature of astrophysical BH candidates and to discover new physics, as in the framework of the standard accretion disk model η cannot exceed 0.32. In Section VI, I discuss the findings of this paper in relation with current estimates of the radiative efficiency of AGN. The conclusions and the issues that need to be addressed before using the most massive objects in AGN to really test the Kerr BH hypothesis are reported in Section VII. In Appendices A and B, the reader can find the non-vanishing metric coefficients respectively of the JP and of the MN metric.

II. ACCRETION DISKS

A. Novikov-Thorne model

The Novikov-Thorne (NT) model is the standard model for accretion disks [26]. It describes geometrically thin and optically thick disks and it is the relativistic generalization of the Shakura-Sunyaev (SS) model [27]. The disk is thin in the sense that the disk opening angle is $h = H/r \ll 1$, where H is the thickness of the disk at the radius r . Magnetic fields are ignored. In the Kerr background, there are four parameters (BH mass M , BH spin parameter a_* , mass accretion rate \dot{M} , and viscosity parameter α), but the model can be easily extended to any (quasi-)stationary, axisymmetric, and asymptotically flat space-time. Accretion is possible because viscous magnetic/turbulent stresses and radiation transport energy and angular momentum outwards. The model assumes that the disk is on the equatorial plane and that the disk’s gas moves on nearly geodesic circular orbits. For long-term accretions, the disk is adjusted on the equatorial plane as a result of the Bardeen-Petterson effect [28]. That remains true even in non-Kerr backgrounds [29]. The assumption of nearly geodesic circular orbits requires that the radial pressure is negligible compared to the gravitational force of the BH. Heat advection is ignored (it scales as $\sim h^2$) and energy is radiated from the disk surface.

The key-ingredient of the NT model is that the inner edge of the disk is at the innermost stable circular orbit (ISCO), where viscous stresses are assumed to vanish. When the gas’s particles reach the ISCO, they quickly plunge into the BH, without emitting additional radiation. At first approximation, the *total efficiency* of the accretion process is

$$\eta_{\text{tot}} = 1 - E_{\text{ISCO}}, \quad (2.1)$$

where E_{ISCO} is the specific energy of the gas at the ISCO radius and depends uniquely on the background geometry. In general, the total power of the accretion process is

converted into radiation and kinetic energy of jet/wind outflows, so we can write $\eta_{\text{tot}} = \eta + \eta_k$. η is the *radiative efficiency* and can be inferred from the bolometric luminosity L_{bol} if the mass accretion rate is known: $L_{\text{bol}} = \eta\dot{M}$. In this paper, I will assume $\eta_k = 0$, i.e. no gravitational energy of the gas is converted to kinetic energy of outflows. This is a conservative assumption for what follows.

As a consequence of the accretion process, the BH spin parameter evolves. Since the gas particles arriving at the ISCO plunge quickly onto the central object, without emission of additional radiation, the BH changes its mass by $\delta M = E_{\text{ISCO}}\delta m$ and its spin angular momentum by $\delta J = L_{\text{ISCO}}\delta m$, where L_{ISCO} is the specific angular momentum of the gas at the ISCO, while δm is the gas rest-mass. The evolution of the spin parameter of the BH turns out to be governed by the following equation:

$$\frac{da_*}{d \ln M} = \frac{1}{M} \frac{L_{\text{ISCO}}}{E_{\text{ISCO}}} - 2a_* . \quad (2.2)$$

If the right hand side of Eq. (2.2) is positive, the accretion process spins the BH up. If it is negative, the BH is spun down. The equilibrium spin parameter a_*^{eq} is reached when the right hand side of Eq. (2.2) vanishes and its value depends on the geometry of the space-time. As discussed in [16] and explained briefly also in Sec. IV, the value of a_*^{eq} we can infer from Eq. (2.2) assuming that all the accreting matter has its angular momentum in the same direction provides the maximum value for the spin parameter of the super-massive BH candidates in galactic nuclei. This fact will be used to get the constraint $a_* < a_*^{\text{eq}}$.

Actually, not all the radiation emitted by the disk can escape to infinity. A part of it leaves the disk, but it is then captured by the BH. Including this effect, Eqs. (2.1) and (2.2) become [30]

$$\eta = 1 - E_{\text{ISCO}} - \zeta_E , \quad (2.3)$$

$$\frac{da_*}{d \ln M} = \frac{1}{M} \frac{L_{\text{ISCO}} + \zeta_L}{E_{\text{ISCO}} + \zeta_E} - 2a_* , \quad (2.4)$$

where ζ_E and ζ_L take into account the radiation captured by the BH and their expression can be found in [30]. There is also a part of radiation that is emitted by the disk and returns to the disk as a consequence of light deflection (returning radiation), interacting with the disk's particles and changing the flux profile emitted by the disk (see e.g. Ref. [31]).

B. Validity of the model

If we relax the assumption of vanishing stresses at the inner edge of the disk, the radiative efficiency increases. The bolometric luminosity of the disk becomes

$$\begin{aligned} L_{\text{bol}} &= \eta\dot{M} = \\ &= g_{\text{ISCO}}\Omega_{\text{ISCO}} + (1 - E_{\text{ISCO}} - \zeta_E)\dot{M} , \end{aligned} \quad (2.5)$$

where g_{ISCO} ($g_{\text{ISCO}} \geq 0$) and Ω_{ISCO} are respectively the torque and the angular velocity of the gas at the ISCO. Another crucial point of the NT model is the α viscosity parameter: magnetic fields, which are thought to drive turbulence in disks, may not behave like a local scalar viscosity. If magnetohydrodynamics torques are present, the radiative efficiency η can even exceed 1, as the flow taps the spin energy of the BH [32]. In this case, it is not easy to recover E_{ISCO} from the estimate of η and even the equilibrium spin parameter a_*^{eq} is not given by Eq. (2.2), but it turns out to be lower [33]. GRMHD simulations show also that the gas's particles may not follow the geodesics of the space-time inside the ISCO [34] and that a significant emission of radiation from the plunging region is possible [35].

So, how good is the NT model to describe the accretion disk around astrophysical BH candidates? For non-magnetized and weakly-magnetized disks, there is a common consensus that the NT model describes correctly thin disks, $h \ll 1$, when the viscosity parameter is small, $\alpha \ll 1$ [36]. A common criterion to select sources with thin disks is that $L_{\text{bol}}/L_{\text{Edd}}$ does not exceed 0.3 [37]. In the case of magnetized disks (in Kerr background, as there are no simulations for other space-times), the issue is still open and controversial. The GRMHD simulations in Ref. [38] (see also [39]) show that the stress at the inner edge of the disk scales as h and the authors conclude that the NT model with vanishing stress boundary condition is recovered for $h \rightarrow 0$. The GRMHD simulations in [35] show instead large stress at the inner edge of the disk even when $h \rightarrow 0$; according to these authors, the NT model cannot describe magnetized disks, even when the disk is very thin. It is not clear if the disagreement between the two groups can be attributed to different configurations of the magnetic fields, different resolution of the simulations, or something else.

III. KERR BLACK HOLES

A Kerr BH is completely specified by two parameters: the mass, M , and the spin parameter, a_* . In the NT model with $\eta_k = 0$, the radiative efficiency of the accretion process η is uniquely determined by the BH spin parameter, as a_* sets the ISCO radius. There is a one-to-one correspondence between a_* and η , and η increases with increasing a_*^2 . At least in principle, an estimate of η could be used to infer the spin parameter of the BH. In practice, assuming the validity of the NT model, we can deduce a lower bound for a_* , as in general $\eta_k \neq 0$.

The radiative efficiency in Kerr background for different values of the BH spin parameter is shown in Tab. I and in the left panel of Fig. 1. If we use Eq. (2.1), for

² That is true only for Kerr BHs, i.e. when $a_* \leq 1$. It is not true in a Kerr background with arbitrary value of the spin parameter [40].

a_*	E_{ISCO}	L_{ISCO}	η	$\Omega_{\text{ISCO}}M$	r_{ISCO}/M
0	$\sqrt{8/9}$	$\sqrt{12}$	$1 - \sqrt{8/9} \approx 0.057$	$1/\sqrt{6^3} \approx 0.068$	6
1	$1/\sqrt{3}$	$2/\sqrt{3}$	$1 - 1/\sqrt{3} \approx 0.423$	1/2	1
0.99614	0.700	1.452	0.300	0.402	1.307
0.99793	0.680	1.395	0.320	0.420	1.240
0.99901	0.660	1.341	0.340	0.438	1.181
0.99960	0.640	1.292	0.360	0.455	1.129
0.99988	0.620	1.246	0.380	0.470	1.084
0.99998	0.600	1.205	0.400	0.484	1.045
0.9978*	0.682	1.400	0.302 (0.318)	0.419	1.246
0.9983*	0.674	1.379	0.308 (0.326)	0.426	1.223
0.9983†	0.674	1.379	0.309 (0.326)	0.426	1.223
0.9986†	0.669	1.365	0.315 (0.331)	0.430	1.207

TABLE I. Kerr space-time. E_{ISCO} , L_{ISCO} , maximum radiative efficiency in the NT model, angular frequency at the ISCO radius, and ISCO radius in Boyer-Lindquist coordinates for different value of the spin parameter. * From Ref. [30], without returning radiation. † From Ref. [31], including returning radiation. See text for details.

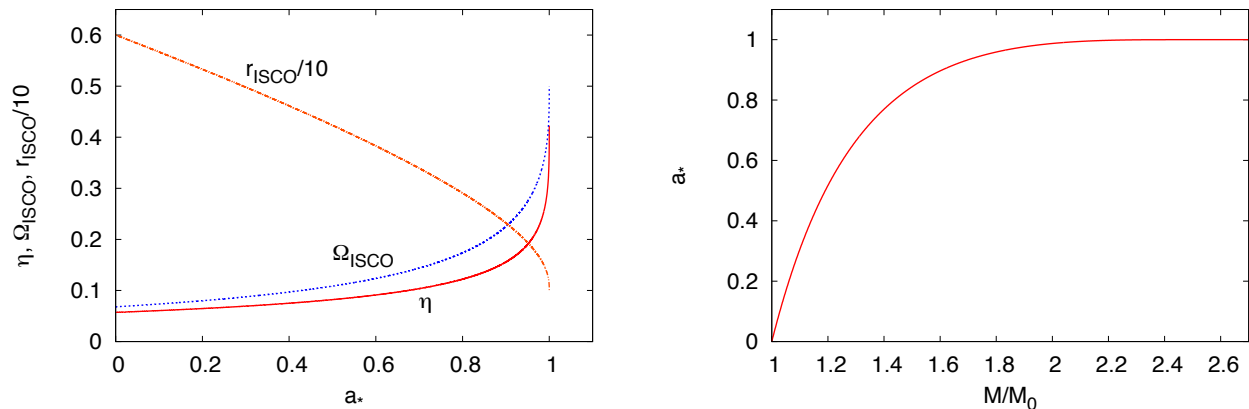


FIG. 1. Kerr space-time. Left panel: maximum radiative efficiency in the NT model, angular frequency at the ISCO radius, and ISCO radius (divided by 10) in Boyer-Lindquist coordinates as a function of the spin parameter. Units $M = 1$. Right panel: Evolution of the spin parameter for an initially non-rotating BH of mass M_0 . See text for details.

corotating accretion disks one finds that η is in the range ~ 0.057 (Schwarzschild BH, $a_* = 0$) to ~ 0.423 (extreme Kerr BH, $a_* = 1$). However, η increases slowly with a_* for low values of the spin parameters and it increases much faster when a_* approaches 1. For instance, $\eta > 0.30$ requires $a_* > 0.996$, $\eta > 0.34$ requires $a_* > 0.999$, and $\eta > 0.40$ demands a_* extremely close to 1 (see Tab. I and Fig. 1).

In the Kerr background, we can analytically integrate Eq. (2.2) and we obtain [41]

$$a_* = \sqrt{\frac{2}{3} \frac{M_0}{M}} \left[4 - \sqrt{18 \frac{M_0^2}{M^2} - 2} \right] \quad (\text{for } M/M_0 \leq \sqrt{6}),$$

$$a_* = 1 \quad (\text{for } M/M_0 > \sqrt{6}), \quad (3.1)$$

for an initially non-rotating BH with mass M_0 . The

equilibrium spin parameter is thus $a_*^{\text{eq}} = 1$, and it is reached after the object increased its mass by a factor $\sqrt{6} \approx 2.4$. The evolution of the spin parameter as a function of M/M_0 is shown in Fig. 1, right panel.

For an astrophysical BH, the situation is slightly different, as there is no realistic mechanism to spin up the object to a_* too close to 1. The accretion process from a thin disk is still a very efficient mechanism, but we have to include the effect of the radiation emitted by the disk and captured by the BH, Eqs. (2.3) and (2.4). In this case, we find slightly lower values for η and a_*^{eq} . However, as η increases very quickly when a_* approaches 1, even a tiny different in a_*^{eq} causes a non-negligible difference in the maximum value of η . As the radiation with angular momentum anti-parallel to the BH spin has larger capture cross section, from Eqs. (2.4) one finds $a_*^{\text{eq}} < 1$. For

instance, Thorne found $a_*^{\text{eq}} = 0.9978$ when the emission of the disk is isotropic, and $a_*^{\text{eq}} = 0.9983$ when the emission is limb-darkened [30]. The corresponding efficiencies [Eq. (2.3)] are respectively 0.302 and 0.308. From Eq. (2.1), we would have found 0.318 (for $a_* = 0.9978$) and 0.326 (for $a_* = 0.9983$). The effect of the returning radiation, which changes a little bit the emission of the disk, introduces an even smaller correction [31]. The equilibrium spin parameter is now $a_*^{\text{eq}} = 0.9983$ in the case of isotropic emission and $a_*^{\text{eq}} = 0.9986$ in the case of limb-darkened emission. The radiative efficiencies turn out to be respectively 0.309 and 0.315 [0.326 and 0.331 if we used Eq. (2.1)]. In conclusion, if the super-massive BH candidates are Kerr BHs, a realistic upper bound for η should be around 0.32, as these objects can unlikely be spun up to a_* higher than roughly 0.998.

Tab. I shows also the angular frequency at the ISCO, Ω_{ISCO} , and the value of the ISCO radius in Boyer-Lindquist coordinates, r_{ISCO} , for the same values of the spin parameter. Even for Ω_{ISCO} and r_{ISCO} there is a one-to-one correspondence (for a given mass M) with the spin parameter of the BH. In the case of corotating disks, the angular frequency at the ISCO increases with a_* , from $\sim 0.068 M$ ($a_* = 0$) to $0.5 M$ ($a_* = 1$). The ISCO radius decreases with a_* , from $6 M$ ($a_* = 0$) to M ($a_* = 1$). Ω_{ISCO} and r_{ISCO} as a function of the spin parameter are shown (for corotating disk) in the left panel of Fig. 1.

IV. JOHANNSEN-PSALTIS SPACE-TIMES

The JP space-times have been proposed in [24] explicitly to be used to test the Kerr geometry around astrophysical BH candidates. They describe BHs (at least for a_* lower than a critical value) and they are an extension of the Kerr solution, in the sense that here the compact objects are specified by the mass, the spin angular momentum, and an infinite number of deformation parameters ϵ_i ($i = 3, 4, 5$, etc.) measuring deviations from the Kerr geometry. When all the deformation parameters vanish, one recovers exactly the Kerr background. The explicit expression of the metric is reported in Appendix A. The JP metric is not a solution of any known gravity theory, but it seems to be a very convenient framework to test the Kerr BH hypothesis.

The NT model for thin accretion disks can be easily extended to non-Kerr backgrounds. The first important difference is the determination of the ISCO radius. In the Kerr background, circular orbits on the equatorial plane are always vertically stable and the ISCO is set by the orbital stability along the radial direction. If the compact object is more oblate than a Kerr BH, that remains true. On the contrary, if the compact object is more prolate (including the case in which the object is still oblate, but simply less oblate than a Kerr BH with the same spin) both kinds of instabilities are possible. When the ISCO radius is marginally stable along the radial direction, as in Kerr, it is at the minimum of the energy of equatorial

circular orbits. When instead the ISCO is marginally stable along the vertical direction, such a minimum does not exist in general. In the latter case, the curve of the energy of equatorial circular orbits around the ISCO is clearly steeper, causing a lower value of E_{ISCO} with respect to the case of radially unstable ISCO with the same radius. The total efficiency η is therefore higher.

As Eqs. (2.2) and (2.4) depend on the geometry of the space-time, the equilibrium spin parameter in these metrics is determined by the deformation parameters ϵ_i . We can notice that in the case of the super-massive BH candidates, a_*^{eq} should be the maximum value for the spin parameter of these objects, independently of their actual nature [16, 29, 42]. Indeed, for the super-massive BH candidates the initial value of a_* , i.e. the one at the time of their birth, is thought to be completely irrelevant, as the mass of these objects has increased by several orders of magnitude from the original one and the spin has evolved accordingly. Long term accretion from a thin disk can efficiently spin the BH up to a_*^{eq} (but it spins the BH down if $a_* > a_*^{\text{eq}}$), while other processes (chaotic accretions, minor and major mergers) more likely spin the object down to $a_* \sim 0$. So, the value of a_*^{eq} we can infer from Eqs. (2.2) and (2.4) can be used to exclude the region $a_* > a_*^{\text{eq}}$ in the diagrams spin parameter vs deformation parameter. This point will be crucial for what follows.

Let us now start considering the properties of the JP space-time with deformation parameter ϵ_3 and $\epsilon_i = 0$ for $i \neq 3$. Fig. 2 shows the efficiency η , as deduced from Eq. (2.1). In particular, we are interested in the most efficient systems and I report the curves on the $a_*\epsilon_3$ -plane with $\eta = 0.30, 0.32, 0.34, 0.36, 0.38, 0.40$. The black solid curve marks the equilibrium spin parameter a_*^{eq} . For $\epsilon_3 > 0$, the compact object is more prolate than Kerr and $a_*^{\text{eq}} < 1$. For $\epsilon_3 < 0$, the object is more oblate and $a_*^{\text{eq}} > 1$. It is thus clear that observations can potentially provide very strong constraints for $\epsilon_3 < 0$, and much weaker bounds for $\epsilon_3 > 0$. In particular, for $\epsilon_3 > 0$, the maximum value of a_* may be even significantly lower than 1, but still η can be very high. Interestingly, for $\epsilon_3 \neq 0$, η does not increase abruptly as a_* approaches a_*^{eq} and therefore the effect of the radiation emitted by the disk and captured by the BH may be neglected. Indeed, we can assume that the radiation captured by the BH decreases a_*^{eq} by ~ 0.002 , as in Kerr (actually the correction to a_*^{eq} should be smaller than 0.002, as the ISCO radius is larger, see the right panel in Fig. 3). This is equivalent to replace the curve of a_*^{eq} in Fig. 2 with the curve $a_*^{\text{eq}} - 0.002$. At this point, we have to decrease η by ~ 0.01 . Except for the Kerr space-time and for the space-times with small deviations from the Kerr geometry, the two effects should not cause significant changes. In particular, we still find a large region with objects with $\eta > 0.32$, which would be impossible for a Kerr BH in a realistic astrophysical context.

Fig. 3 shows the contour plot of the angular frequency at the ISCO, Ω_{ISCO} , (left panel) and the one of

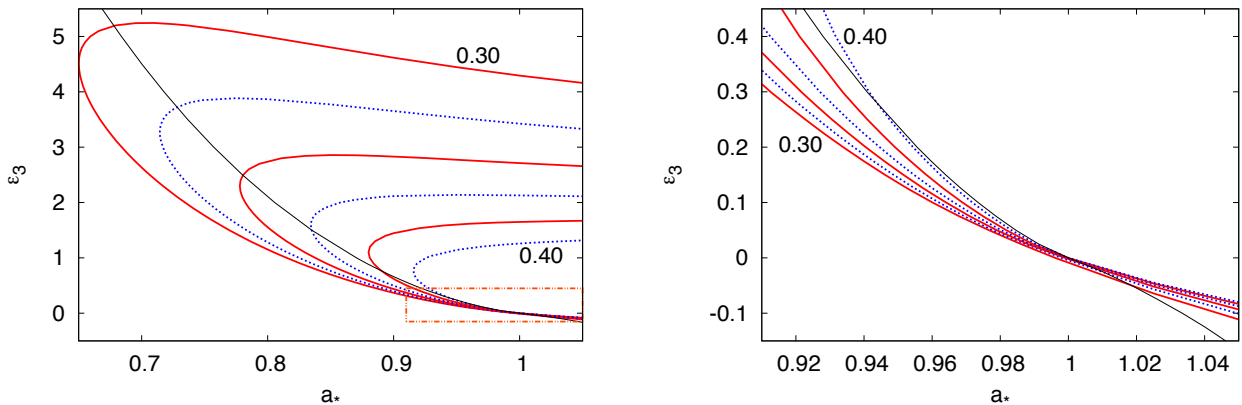


FIG. 2. JP space-time with deformation parameter ϵ_3 and $\epsilon_i = 0$ for $i \neq 3$. Contour plots of the radiative efficiency $\eta = 1 - E_{\text{ISCO}}$: $\eta = 0.30$ (red solid curve), 0.32 (blue dotted curve), 0.34 (red solid curve), 0.36 (blue dotted curve), 0.38 (red solid curve), 0.40 (blue dotted curve). The black solid curve is the equilibrium spin parameter a_*^{eq} as inferred from Eq. (2.2) and represents the maximum value for the spin parameter of the super-massive BH candidates. This means that the region with $a_* > a_*^{\text{eq}}$ is not allowed. The right panel is simply the enlargement of the area inside the orange box in the left panel.

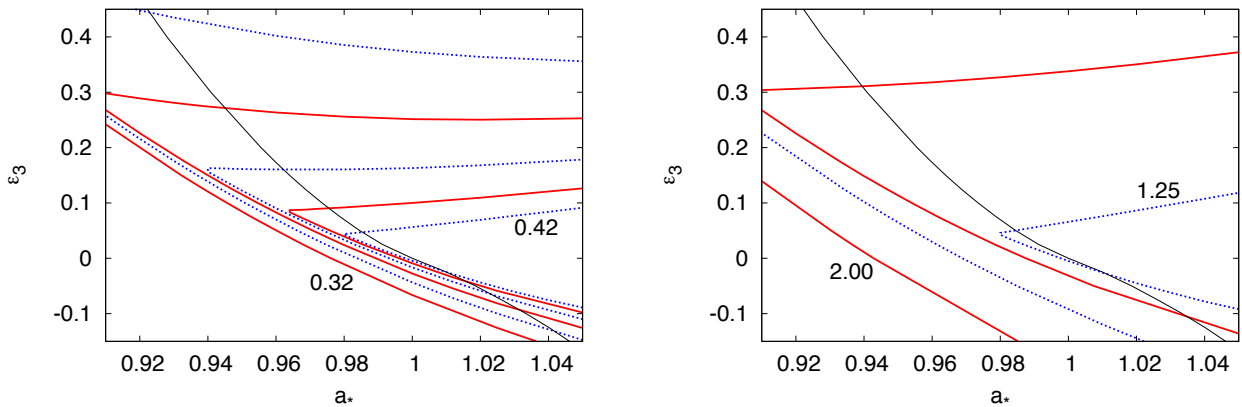


FIG. 3. JP space-time with deformation parameter ϵ_3 and $\epsilon_i = 0$ for $i \neq 3$. Left panel: contour plot of the angular frequency at the ISCO radius: $\Omega_{\text{ISCO}}/M = 0.32$ (red solid curve), 0.34 (blue dotted curve), 0.36 (red solid curve), 0.38 (blue dotted curve), 0.40 (red solid curve), 0.42 (blue dotted curve). Right panel: contour plot of the ISCO radius in Boyer-Lindquist coordinates: $r_{\text{ISCO}}/M = 2.00$ (red solid curve), 1.75 (blue dotted curve), 1.50 (red solid curve), 1.25 (blue dotted curve). The black solid curve is the equilibrium spin parameter a_*^{eq} as inferred from Eq. (2.2).

the ISCO radius in Boyer-Lindquist coordinates, r_{ISCO} , (right panel). While accretion in JP space-time may have high efficiency, thus mimicking a Kerr BH with a_* extremely close to 1 (or even exceeding the efficiency of a Kerr BH with $a_* = 1$), the same object would have Ω_{ISCO} and r_{ISCO} more similar to the one expected for Kerr BHs with lower spin parameter. Ω_{ISCO} can be potentially inferred in several ways from observations (e.g. from the variability of the source) and that may be useful to break the degeneracy between a_* and ϵ_3 in η .

Lastly, we can consider JP backgrounds with a different deformation parameter. Interestingly, one finds essentially the same picture. In Fig. 4, I report the contour plots of η for the JP space-time with deformation

parameter ϵ_4 and $\epsilon_i = 0$ for $i \neq 4$ (left panel) and for the one with deformation parameter ϵ_5 and $\epsilon_i = 0$ for $i \neq 5$ (right panel). For these two cases, even the contour plots of Ω_{ISCO} and r_{ISCO} (not shown here) are fairly similar to the ones in Fig. 3.

V. MANKO-NOVIKOV SPACE-TIMES

The MN space-times are stationary, axisymmetric, and asymptotically flat exact solutions of the Einstein's vacuum equations [25]. These metrics can describe the exterior gravitational field of a compact object with mass M , spin parameter a_* , and arbitrary mass-multipole mo-

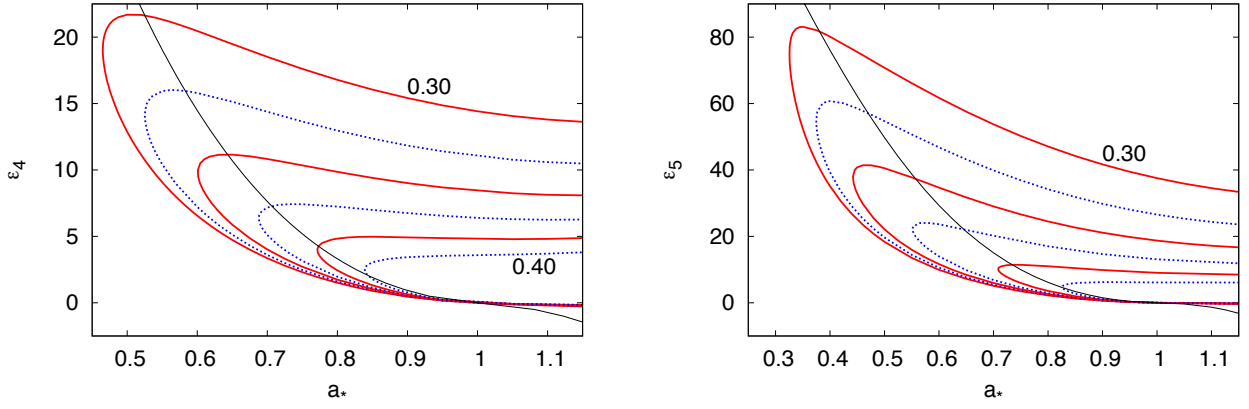


FIG. 4. As in Fig. 2, for the JP space-time with deformation parameter ϵ_4 and $\epsilon_i = 0$ for $i \neq 4$ (left panel) and for the one with deformation parameter ϵ_5 and $\epsilon_i = 0$ for $i \neq 5$ (right panel).

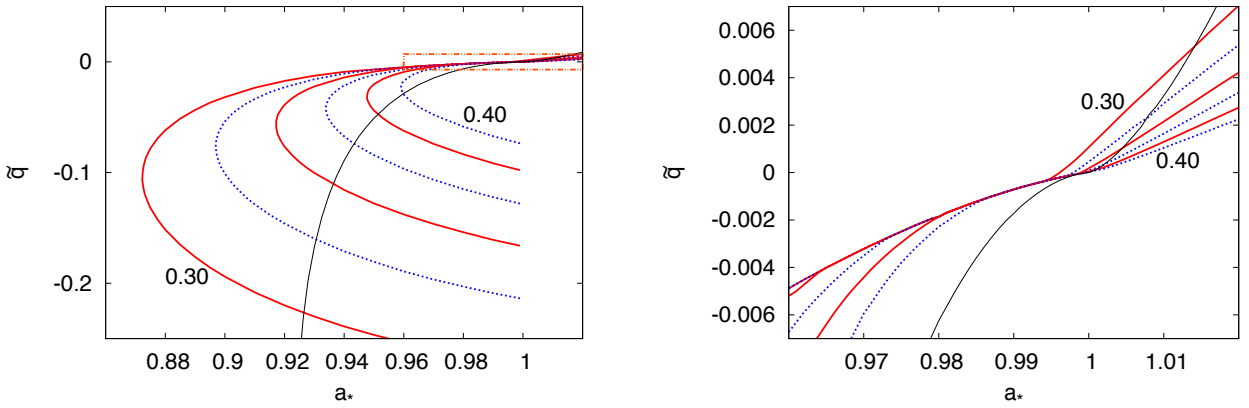


FIG. 5. As in Fig. 2 for the MN space-time with deformation parameter \tilde{q} . The compact object is oblate (prolate) when $\tilde{q} > -1$ ($\tilde{q} < -1$), but it is more oblate (prolate) than a Kerr BH with the same value of the spin parameter for $\tilde{q} > 0$ ($\tilde{q} < 0$).

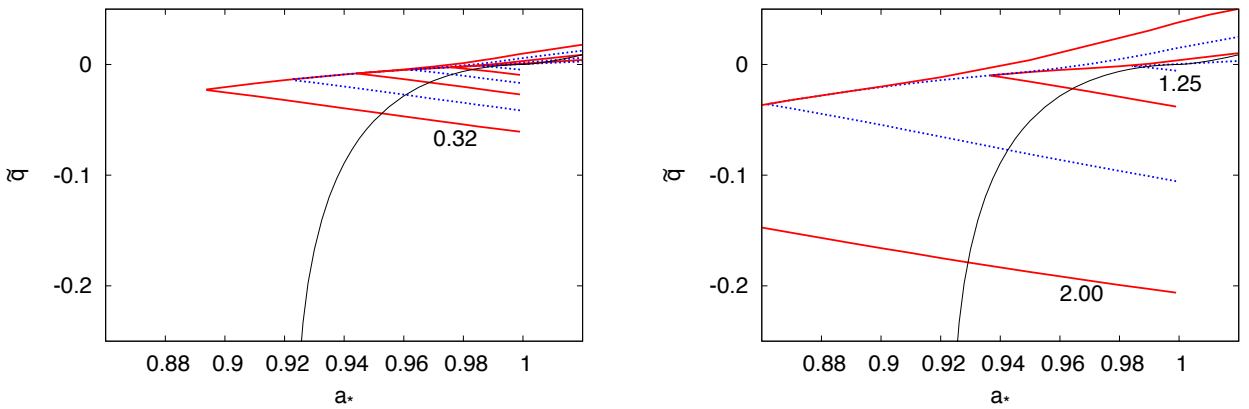


FIG. 6. As in Fig. 3 for the MN space-time with deformation parameter \tilde{q} .

ments, while the current-multipole moments are fixed by the former. The simplest non-Kerr object has three free parameters: mass M , spin parameter a_* , and anomalous quadrupole moment \tilde{q} (see Appendix B). \tilde{q} is defined by

$$Q = (1 + \tilde{q})Q_{\text{Kerr}}, \quad (5.1)$$

where Q is the mass-quadrupole moment of the compact object, while $Q_{\text{Kerr}} = -a_*^2 M^3$ is the one of a Kerr BH with the same spin parameter a_* . The case $\tilde{q} = 0$ corresponds to the Kerr metric, while for $\tilde{q} > 0$ ($\tilde{q} < 0$) the object is more oblate (prolate) than a Kerr BH. The properties of this subclass of MN space-times with deformation parameter \tilde{q} were studied in [43] and [18]. When $\tilde{q} < 0$, for a quite restricted set of values of a_* and \tilde{q} , the plunging region does not connect the ISCO to the compact object [18]. That occurs when inside the ISCO there is another region with stable circular orbits on the equatorial plane and energy lower than E_{ISCO} . In these space-times, the gas's particles plunging from the ISCO get trapped between the ISCO and the compact object. As the gas need to radiate additional energy and angular momentum in order to fall to the compact object, the value of the radiative efficiency turns out to be higher than the one inferred from Eq. (2.1) or Eq. (2.3). The actual value of η depends on the astrophysical processes. For instance, Ref. [18] discussed a simple model in which the gas forms a thick disk inside the ISCO and $\eta = 1 - E_{\text{in}}$, where E_{in} is the specific energy at the inner edge of the thick disk, is up to a few percent higher than the one predicted by Eq. (2.1).

Fig. 5 shows the radiative efficiency η as computed from Eq. (2.1). The MN metric is written in prolate spheroidal coordinates, which require $a_* < 1$; here the region $a_* \geq 1$ is covered by the Malko-Mielke-Sanabria Gómez solution [44] which can be parametrized by the same three parameters of our subclass of the MN metric (i.e. M , a_* , and \tilde{q}) and was shown to be very similar to the MN space-time in the common region of validity [42]. It is clear that there are strong analogies with the JP space-times. For objects more oblate than Kerr, $a_*^{\text{eq}} > 1$ and a high radiative efficiency is possible only for small deviations from the Kerr geometry. For objects more prolate than Kerr, $a_*^{\text{eq}} < 1$ and when the ISCO radius is set by the orbital stability along the vertical direction η can be high even for objects rotating slower. Fig. 6 shows the angular frequency at the ISCO, Ω_{ISCO} , and the ISCO radius in Boyer-Lindquist coordinates, r_{ISCO} . As in the JP background, the same object with high radiative efficiency has lower Ω_{ISCO} and larger r_{ISCO} . The case of the MN space-time with $\tilde{q} = 0$ and an anomalous mass-hexadecapole moment \tilde{h} shows similar properties in η , Ω_{ISCO} , and r_{ISCO} .

VI. DISCUSSION

The radiative efficiency of a source can be deduced from the formula $\eta = L_{\text{bol}}/\dot{M}$. In general, however,

it is not easy to get an estimate of η , because a measurement of the mass accretion rate can be problematic. The Soltan's argument provides an elegant way to determine the mean radiative efficiency of AGN, $\bar{\eta}$, from the mean BH mass density in the contemporary Universe and the AGN luminosity per unit volume integrated over time [20]. There are several sources of uncertainty in the final result, but a conservative bound seems to be $\bar{\eta} > 0.15$ [21]. If the compact objects in AGN are Kerr BHs, this constraint requires $\bar{a}_* > 0.89$. In Ref. [22], the authors used a revised version of the Soltan's argument, in which some important assumptions are not necessary. They found a mean radiative efficiency $\bar{\eta} \approx 0.30 - 0.35$ in the redshift interval $0.4 < z < 2.1$.

Recently, it has been proposed a way to estimate the radiative efficiency of individual AGN [23]. The mass accretion rate \dot{M} can indeed be determined from the low frequency region of the thermal spectrum of the accretion disk of these objects, if the mass M is known. The standard accretion disk model cannot reproduce the observed spectrum of AGN. That is due to reprocessing, Comptonization in a corona, radiative transfer effects in the inner accretion disk, and so on. Here the key-point is that this method relies on the validity of the simple thin-disk model at relatively large radii, where these effects are thought to be irrelevant. One can then estimate the total luminosity of the source, irrespective of its exact production mechanism, and infer the radiative efficiency. So, the redistribution of the radiation emitted in the accretion process does not affect the measurement of radiative efficiency; for more details, see Sections 2.3 and 4.3 of Ref. [23]. The authors found a strong correlation of η with M , raising from $\eta \sim 0.03$ when $M \sim 10^7 M_{\odot}$ and $L_{\text{bol}}/L_{\text{Edd}} \sim 1$ to $\eta \sim 0.4$ when $M \sim 10^9 M_{\odot}$ and $L_{\text{bol}}/L_{\text{Edd}} \sim 0.3$.

The most massive objects in AGN with $M \sim 10^9 M_{\odot}$ may be excellent candidates to test the Kerr BH hypothesis. The standard criterion to consider thin disks is indeed that $L_{\text{bol}}/L_{\text{Edd}}$ does not exceed 0.3, corresponding to an opening angle h not larger than 0.05. In this case, the estimate of η may provide a measurement of the specific energy at the ISCO (or at least a lower bound, as we are neglecting η_{K} and ζ_{E}). The estimate of η can then be used to constrain possible deviations from the Kerr geometry and may have some advantages with respect to the most popular techniques to measure the BH spin parameter, i.e. the continuum fitting method and the $\text{K}\alpha$ iron line analysis. The continuum fitting method can be used only for stellar-mass BH candidates, for which there is no argument to constrain a_* : the value of the spin parameter of the BH candidates in X-ray binary systems should reflect the one at the time of the formation of the object and it is definitively impossible to predict its value relaxing the assumption that GR is the correct theory of gravity. The method of the $\text{K}\alpha$ iron line can be used for the super-massive BH candidates in galactic nuclei (so we can impose $a_* < a_*^{\text{eq}}$), but it necessarily relies on an ad hoc intrinsic surface brightness profile and there is no

way to determine it a priori. Although simulations have the potential to compute the surface brightness profile, the standard required to test the Kerr background is a much higher level of reliability than is likely to be met at any time in the foreseeable future.

Let us now assume that future GRMHD simulations confirm the validity of the NT model for thin accretion disks and that future observations provide robust evidence that the most massive objects in AGN have a very high radiative efficiency and a moderate mass accretion rate. If we exclude the possibility of objects more prolate than Kerr, which may be difficult to explain theoretically³, from the right panel of Fig. 5 we can see that \tilde{q} can be constrained at the level of $\sim 10^{-3}$. That roughly corresponds to test the mass-quadrupole moment of these objects with a precision $\sim 10^{-3}$, see Eq. (5.1). For a self-gravitating fluid with reasonable equations of state, \tilde{q} is much larger, i.e. the compact object becomes significantly more oblate than a Kerr BH when the spin parameter increases. For instance, a neutron star should have $\tilde{q} > 1$ [45]. A similar bound may be obtained by observing the gravitational waves emitted by an EMRI with future space-based gravitational-wave detectors (see the third reference in [11]), even if a direct comparison is not possible, as here we are probing the geometry of the space-time very close to the compact objects, where higher orders multipole moments are not really negligible, while gravitational wave detectors will study the space-time at larger distances, and therefore they will be sensitive to the mass-quadrupole moment only. If we do not exclude a priori the existence of compact objects more prolate than a Kerr BH, the constraint is much weaker: for $\eta > 0.30$, deviations from the Kerr mass-quadrupole moments can still be up to 20%. Let us now consider a more exotic situation: the NT model works and observations find unambiguously $\eta > 0.32$. In absence of torque at the inner edge of the disk, it would be difficult to explain this outcome in the Kerr background, and new physics may be invoked. Let us notice, however, that a non-Kerr background can explain high η , say up to $\eta \sim 0.4$, but higher values may not be natural, as we still have $a_* < a_*^{\text{eq}}$.

³ The true problem is not the existence of compact objects less oblate than a Kerr BH with the same spin parameter, but that the objects we are talking about have the ISCO marginally stable along the vertical direction. In the case of the JP metric, these objects are BHs with two disconnected event horizons, one above and one below the equatorial plane [19]. These objects more prolate than Kerr and high radiative efficiency have therefore “two centers of attraction”, one above and one below the equatorial plane. It is not clear at all if such a system can exist and be stable.

VII. CONCLUSIONS

There is some evidence that the most massive BH candidates in AGN have a high radiative efficiency and a thin accretion disk. In this case, they could be excellent candidates to test GR in the strong field regime and, in particular, the Kerr BH paradigm. A robust observation of a high radiative efficiency together with the confirmation of the validity of the standard accretion disk model for the accretion process onto these objects would constrain possible deviations from the Kerr geometry of the space-time around astrophysical BH candidates. If we restrict our attention only to objects more oblate than a Kerr BH with the same spin parameter, a radiative efficiency $\eta > 0.30$ requires that the quadrupole moment of the compact object deviates not more than $\sim 10^{-3}$ with respect to the one of a Kerr BH. If we allow for the existence of compact objects more prolate than a Kerr BH (whose existence, however, may be questionable, see the footnote 3), the constraints is much weaker, at the level of 20%. On the other hand, the observation of an accreting BH candidate with $\eta > 0.32$ might indicate that the super-massive BH candidates in galactic nuclei are not the Kerr BH of GR, as there is no realistic astrophysical mechanism capable to spin up them to $a_* > 0.998$.

For the time being, there are at least two main issues to address before using the measurement of the radiative efficiency of individual AGN to test GR:

1. We do not really know if the NT model can describe thin accretion disks around astrophysical BH candidates. If it can or it is easy to estimate the necessary corrections, the measurement of η could provide an interesting way to probe the geometry of the space-time around BH candidates. If it cannot, it seems to be impossible to test GR (with this or other approaches) from the properties of the radiation emitted by the gas in the accretion disk and we should wait for the advent of gravitational wave astronomy.
2. We need robust and more precise measurements of η . At present, there are several sources with $\eta > 0.32$ at high masses, but we cannot really exclude they actually have $\eta < 0.32$ [23]. There are some sources of uncertainty in the final estimate of the radiative efficiency and the most important one is the determination of the mass of the BH candidate. Moreover, the results presented in [23] are based on a preliminary study and it is necessary to further investigate and verify the validity of the method proposed by these authors.

ACKNOWLEDGMENTS

This work was supported by the Humboldt Foundation.

Appendix A: JP metric

The JP metric is not a solution in any known gravity theory. It is a simple parametrization to describe the space-time around non-Kerr BHs and was specifically proposed to test the Kerr BH hypothesis [24]. The metric was obtained by starting from a deformed Schwarzschild solution and then by applying a Newman-Janis transformation. The non-zero metric coefficients in Boyer-Lindquist coordinates are:

$$\begin{aligned}
g_{tt} &= -\left(1 - \frac{2Mr}{\rho^2}\right)(1+h), \\
g_{t\phi} &= -\frac{2aMr \sin^2 \theta}{\rho^2}(1+h), \\
g_{\phi\phi} &= \sin^2 \theta \left[r^2 + a^2 + \frac{2a^2 Mr \sin^2 \theta}{\rho^2} \right] + \\
&\quad + \frac{a^2(\rho^2 + 2Mr) \sin^4 \theta}{\rho^2} h, \\
g_{rr} &= \frac{\rho^2(1+h)}{\Delta + a^2 h \sin^2 \theta}, \\
g_{\theta\theta} &= \rho^2,
\end{aligned} \tag{A1}$$

where

$$\begin{aligned}
\rho^2 &= r^2 + a^2 \cos^2 \theta, \\
\Delta &= r^2 - 2Mr + a^2, \\
h &= \sum_{k=0}^{\infty} \left(\epsilon_{2k} + \frac{Mr}{\rho^2} \epsilon_{2k+1} \right) \left(\frac{M^2}{\rho^2} \right)^k.
\end{aligned} \tag{A2}$$

The metric has an infinite number of free parameters ϵ_i and the Kerr solution is recovered when all these parameters are set to zero. However, in order to recover the

correct Newtonian limit we have to impose $\epsilon_0 = \epsilon_1 = 0$, while ϵ_2 is constrained at the level of 10^{-4} from current tests in the Solar System [24].

Appendix B: MN metric

The MN metric is a stationary, axisymmetric, and asymptotically flat exact solution of the Einstein's vacuum equations with arbitrary mass-multipole moments [25]. It does not describe the space-time around a BH and it has naked singularities and closed time-like curves at small radii. These pathological features should be either inside some sort of exotic compact object, whose exterior gravitational field would be described by the MN metric, or GR should break down close to them. The non-zero metric coefficients in prolate spheroidal coordinates are:

$$\begin{aligned}
g_{tt} &= -f, \\
g_{t\phi} &= f\omega, \\
g_{\phi\phi} &= \frac{k^2}{f} (x^2 - 1)(1 - y^2) - f\omega^2, \\
g_{xx} &= \frac{k^2 e^{2\gamma}}{f} \frac{x^2 - y^2}{x^2 - 1}, \\
g_{yy} &= \frac{k^2 e^{2\gamma}}{f} \frac{x^2 - y^2}{1 - y^2},
\end{aligned} \tag{B1}$$

where

$$\begin{aligned}
f &= e^{2\psi} A/B, \\
\omega &= 2ke^{-2\psi} CA^{-1} - 4k\alpha(1 - \alpha^2)^{-1}, \\
e^{2\gamma} &= e^{2\gamma'} A(x^2 - 1)^{-1} (1 - \alpha^2)^{-2},
\end{aligned} \tag{B2}$$

and

$$\begin{aligned}
\psi &= \sum_{n=1}^{+\infty} \frac{\alpha_n P_n}{R^{n+1}}, \\
\gamma' &= \frac{1}{2} \ln \frac{x^2 - 1}{x^2 - y^2} + \sum_{m,n=1}^{+\infty} \frac{(m+1)(n+1)\alpha_m \alpha_n}{(m+n+2)R^{m+n+2}} (P_{m+1} P_{n+1} - P_m P_n) + \\
&\quad + \left[\sum_{n=1}^{+\infty} \alpha_n \left((-1)^{n+1} - 1 + \sum_{k=0}^n \frac{x-y + (-1)^{n-k}(x+y)}{R^{k+1}} P_k \right) \right], \\
A &= (x^2 - 1)(1 + ab)^2 - (1 - y^2)(b - a)^2, \\
B &= [x + 1 + (x - 1)ab]^2 + [(1 + y)a + (1 - y)b]^2, \\
C &= (x^2 - 1)(1 + ab)[b - a - y(a + b)] + (1 - y^2)(b - a)[1 + ab + x(1 - ab)], \\
a &= -\alpha \exp \left[\sum_{n=1}^{+\infty} 2\alpha_n \left(1 - \sum_{k=0}^n \frac{(x-y)}{R^{k+1}} P_k \right) \right], \\
b &= \alpha \exp \left[\sum_{n=1}^{+\infty} 2\alpha_n \left((-1)^n + \sum_{k=0}^n \frac{(-1)^{n-k+1}(x+y)}{R^{k+1}} P_k \right) \right].
\end{aligned} \tag{B3}$$

Here $R = \sqrt{x^2 + y^2 - 1}$ and P_n are the Legendre polynomials with argument xy/R ,

$$P_n = P_n\left(\frac{xy}{R}\right),$$

$$P_n(\chi) = \frac{1}{2^n n!} \frac{d^n}{d\chi^n} (\chi^2 - 1)^n. \quad (\text{B4})$$

The standard Boyer-Lindquist coordinates (r, θ) are related to the prolate spheroidal coordinates (x, y) by

$$r = kx + M,$$

$$\cos \theta = y. \quad (\text{B5})$$

The MN solution has an infinite number of free parameters: k , which regulates the mass of the space-time; α , which regulates the spin; and α_n ($n = 1, \dots, +\infty$) which regulates the mass-multipole moments, starting from the dipole α_1 , to the quadrupole α_2 , etc. For $\alpha \neq 0$ and $\alpha_n = 0$, the MN solution reduces to the Kerr metric. For $\alpha = \alpha_n = 0$, it reduces to the Schwarzschild solution. For $\alpha = 0$ and $\alpha_n \neq 0$, one obtains the static Weyl metric. Without loss of generality, we can put $\alpha_1 = 0$ to bring the massive object to the origin of the coordinate system. The simplest extension of the Kerr solution is

thus the subclass of MN space-times with $\alpha_n = 0$ for $n \neq 2$. Here there are three free parameters (k , α , and α_2) related to the mass M , the dimensionless spin parameter $a_* = J/M^2$, and the dimensionless anomalous quadrupole moment \tilde{q} , defined by $Q = -(1 + \tilde{q})a_*^2 M^3$, with Q the mass-quadrupole moment of the object, by the relations

$$\alpha = \frac{\sqrt{1 - a_*^2} - 1}{a_*},$$

$$k = M \frac{1 - \alpha^2}{1 + \alpha^2},$$

$$\alpha_2 = \tilde{q} a_*^2 \frac{M^3}{k^3}. \quad (\text{B6})$$

Note that \tilde{q} measures the deviation from the quadrupole moment of a Kerr BH. In particular, since $Q_{\text{Kerr}} = -a_*^2 M^3$, the solution is oblate (prolate) for $\tilde{q} > -1$ ($\tilde{q} < -1$), but it is more oblate (prolate) than the Kerr one for $\tilde{q} > 0$ ($\tilde{q} < 0$). When $\tilde{q} = 0$, the solution reduces to the Kerr metric, but when $\tilde{q} \neq 0$ also the higher-order mass-multipole moments have a different value than in Kerr.

-
- [1] C. M. Will, Living Rev. Rel. **9**, 3 (2006) [gr-qc/0510072].
- [2] E. Fischbach and C. L. Talmadge, *The search for non-Newtonian gravity*, (Springer, New York, New York, 1999).
- [3] R. Penrose, Riv. Nuovo Cim. **1**, 252 (1969) [Gen. Rel. Grav. **34**, 1141 (2002)].
- [4] B. Carter, Phys. Rev. Lett. **26**, 331 (1971); D. C. Robinson, Phys. Rev. Lett. **34**, 905 (1975).
- [5] R. Narayan, New J. Phys. **7**, 199 (2005) [gr-qc/0506078].
- [6] V. Kalogera and G. Baym, Astrophys. J. **470**, L61 (1996) [astro-ph/9608059].
- [7] E. Maoz, Astrophys. J. **494**, L181 (1998) [astro-ph/9710309].
- [8] R. Narayan and J. E. McClintock, New Astron. Rev. **51**, 733 (2008) [arXiv:0803.0322 [astro-ph]]; A. E. Broderick, A. Loeb and R. Narayan, Astrophys. J. **701**, 1357 (2009) [arXiv:0903.1105 [astro-ph.HE]].
- [9] M. A. Abramowicz, W. Kluzniak and J. -P. Lasota, Astron. Astrophys. **396**, L31 (2002) [astro-ph/0207270].
- [10] C. Bambi, Mod. Phys. Lett. A **26**, 2453 (2011) [arXiv:1109.4256 [gr-qc]].
- [11] F. D. Ryan, Phys. Rev. D **52**, 5707 (1995); K. Glampedakis and S. Babak, Class. Quant. Grav. **23**, 4167 (2006) [gr-qc/0510057]. L. Barack and C. Cutler, Phys. Rev. D **75**, 042003 (2007) [gr-qc/0612029]; T. A. Apostolatos, G. Lukes-Gerakopoulos and G. Contopoulos, Phys. Rev. Lett. **103**, 111101 (2009) [arXiv:0906.0093 [gr-qc]].
- [12] C. Bambi and E. Barausse, Astrophys. J. **731**, 121 (2011) [arXiv:1012.2007 [gr-qc]].
- [13] D. Psaltis and T. Johannsen, arXiv:1011.4078 [astro-ph.HE].
- [14] T. Johannsen and D. Psaltis, Astrophys. J. **726**, 11 (2011) [arXiv:1010.1000 [astro-ph.HE]].
- [15] C. Bambi, Phys. Rev. D **83**, 103003 (2011) [arXiv:1102.0616 [gr-qc]].
- [16] C. Bambi, Phys. Lett. B **705**, 5 (2011) [arXiv:1110.0687 [gr-qc]].
- [17] C. Bambi and K. Freese, Phys. Rev. D **79**, 043002 (2009) [arXiv:0812.1328 [astro-ph]]; C. Bambi and N. Yoshida, Class. Quant. Grav. **27**, 205006 (2010) [arXiv:1004.3149 [gr-qc]]; C. Bambi, F. Caravelli and L. Modesto, arXiv:1110.2768 [gr-qc].
- [18] C. Bambi and E. Barausse, Phys. Rev. D **84**, 084034 (2011) [arXiv:1108.4740 [gr-qc]].
- [19] C. Bambi and L. Modesto, Phys. Lett. B **706**, 13 (2011) [arXiv:1107.4337 [gr-qc]].
- [20] A. Soltan, Mon. Not. Roy. Astron. Soc. **200**, 115 (1982).
- [21] M. Elvis, G. Risaliti and G. Zamorani, Astrophys. J. **565**, L75 (2002) [astro-ph/0112413].
- [22] J. -M. Wang, Y. -M. Chen, L. C. Ho and R. J. McLure, Astrophys. J. **642**, L111 (2006) [astro-ph/0603813].
- [23] S. W. Davis and A. Laor, Astrophys. J. **728**, 98 (2011) [arXiv:1012.3213 [astro-ph.CO]].
- [24] T. Johannsen and D. Psaltis, Phys. Rev. D **83**, 124015 (2011) [arXiv:1105.3191 [gr-qc]].
- [25] V. S. Manko and I. D. Novikov, Class. Quant. Grav. **9**, 2477 (1992).
- [26] I. D. Novikov, K. S. Thorne, "Astrophysics of Black Holes" in *Black Holes*, edited by C. De Witt and B. De Witt (Gordon and Breach, New York, New York, 1973), pp. 343-450; D. N. Page and K. S. Thorne, Astrophys. J. **191**, 499 (1974).
- [27] N. I. Shakura and R. A. Sunyaev, Astron. Astrophys. **24**, 337 (1973).

- [28] J. M. Bardeen and J. A. Petterson, *Astrophys. J.* **195**, L65 (1975).
- [29] C. Bambi, *Europhys. Lett.* **94**, 50002 (2011) [arXiv:1101.1364 [gr-qc]].
- [30] K. S. Thorne, *Astrophys. J.* **191**, 507 (1974).
- [31] L. -X. Li, E. R. Zimmerman, R. Narayan and J. E. McClintock, *Astrophys. J. Suppl.* **157**, 335 (2005) [astro-ph/0411583].
- [32] E. Agol and J. Krolik, *Astrophys. J.* **528**, 161 (2000) [astro-ph/9908049]; A. Tchekhovskoy, R. Narayan and J. C. McKinney, arXiv:1108.0412 [astro-ph.HE].
- [33] C. F. Gammie, S. L. Shapiro and J. C. McKinney, *Astrophys. J.* **602**, 312 (2004) [astro-ph/0310886].
- [34] J. H. Krolik, *Astrophys. J.* **515**, L73 (1999) [astro-ph/9902267].
- [35] S. C. Noble and J. H. Krolik, *Astrophys. J.* **703**, 964 (2009) [arXiv:0907.1655 [astro-ph.HE]]; S. C. Noble, J. H. Krolik and J. F. Hawley, *Astrophys. J.* **711**, 959 (2010) [arXiv:1001.4809 [astro-ph.HE]].
- [36] N. Afshordi and B. Paczynski, *Astrophys. J.* **592**, 354 (2003) [astro-ph/0202409].
- [37] J. E. McClintock, R. Shafee, R. Narayan, R. A. Remillard, S. W. Davis and L. -X. Li, *Astrophys. J.* **652**, 518 (2006) [astro-ph/0606076].
- [38] R. F. Penna, J. C. McKinney, R. Narayan, A. Tchekhovskoy, R. Shafee and J. E. McClintock, *Mon. Not. Roy. Astron. Soc.* **408**, 752 (2010) [arXiv:1003.0966 [astro-ph.HE]].
- [39] R. F. Penna, A. Sadowski and J. C. McKinney, arXiv:1110.6556 [astro-ph.HE].
- [40] R. Takahashi and T. Harada, *Class. Quant. Grav.* **27**, 075003 (2010) [arXiv:1002.0421 [astro-ph.HE]].
- [41] J. M. Bardeen, *Nature* **226**, 64 (1970).
- [42] C. Bambi, *JCAP* **1105**, 009 (2011) [arXiv:1103.5135 [gr-qc]].
- [43] J. R. Gair, C. Li and I. Mandel, *Phys. Rev. D* **77**, 024035 (2008) [arXiv:0708.0628 [gr-qc]].
- [44] V. S. Manko, E. W. Mielke and J. D. Sanabria-Gomez, *Phys. Rev. D* **61**, 081501 (2000) [gr-qc/0001081]; V. S. Manko, J. D. Sanabria-Gomez and O. V. Manko, *Phys. Rev. D* **62**, 044048 (2000).
- [45] W. G. Laarakkers and E. Poisson, *Astrophys. J.* **512**, 282 (1999) [gr-qc/9709033].